Title
Neuregulin and ErbB expression is regulated by development and sensory experience in mouse visual cortex.

Journal
The Journal of comparative neurology, 528(3)

ISSN
0021-9967

Authors
Grieco, Steven F
Wang, Gina
Mahapatra, Ananya
et al.

Publication Date
2020-02-01

DOI
10.1002/cne.24762

HHS Public Access

Author manuscript

J Comp Neurol. Author manuscript; available in PMC 2021 February 15.

Published in final edited form as:

J Comp Neurol. 2020 February 15; 528(3): 419–432. doi:10.1002/cne.24762.

Neuregulin and ErbB expression is regulated by development and sensory experience in mouse visual cortex

Steven F. Grieco[1], **Gina Wang**[1], **Ananya Mahapatra**[1], **Cary Lai**[2], **Todd C. Holmes**[3], **Xiangmin Xu**[1,4]

[1]Department of Anatomy and Neurobiology, School of Medicine, University of California, Irvine, CA, 92697-1275

[2]Department of Psychological and Brain Sciences, Indiana University, Bloomington, IN, 47405-7000

[3]Department of Physiology and Biophysics, School of Medicine, University of California, Irvine, CA, 92697-4560

[4]Department of Biomedical Engineering, University of California, Irvine, CA, 92697-2715

Abstract

Neuregulins (NRGs) are protein ligands that impact neural development and circuit function. NRGs signal through the ErbB receptor tyrosine kinase family. NRG1/ErbB4 signaling in parvalbumin-expressing (PV) inhibitory interneurons is critical for visual cortical plasticity. There are multiple types of NRGs and ErbBs that can potentially contribute to visual cortical plasticity at different developmental stages. Thus, it is important to understand the normal developmental expression profiles of NRGs and ErbBs in specific neuron types in the visual cortex, and to study whether and how their expression changes in PV inhibitory neurons and excitatory neurons track with sensory perturbation. Cell type specific translating ribosome affinity purification (TRAP) and qPCR was used to compare mRNA expression of *nrg1,2,3,4* and *erbB1,2,3,4* in PV and excitatory neurons in visual cortex. We show that the expression of *nrg1* and *nrg3* decreases in PV neurons at the critical period peak, postnatal day 28 (P28) after monocular deprivation and dark rearing, and in the adult cortex (at P104) after 2-week long dark exposure. In contrast, *nrg1* expression by excitatory neurons is unchanged at P28 and P104 following sensory deprivation, whereas *nrg3* expression by excitatory neurons shows changes depending on the age and the mode of sensory deprivation. ErbB4 expression in PV neurons remains consistently high and does not appear to change in response to sensory deprivation. These data provide new important details of cell type specific NRG/ErbB expression in the visual cortex and support that NRG1/ErbB4 signaling is implicated in both critical period and adult visual cortical plasticity.

Address all manuscript correspondence to: Dr. Xiangmin Xu, Department of Anatomy and Neurobiology, School of Medicine, University of California, Irvine, CA, 92697-1275, Tel: 949.824.0040, xiangmix@uci.edu.

Author contributions: S.F.G., A.M., and G.W. performed experiments. S.F.G., C.L., T.C.H., and X.X. analyzed the data and wrote the paper. S.F.G., T.C.H. and X.X. designed the research and wrote the paper.

Data Availability Statement

The data that support the findings of this study are available from the corresponding author upon reasonable request.

Statement of conflict of interests

All authors disclose no conflict of interests for this work.

Graphical Abstract

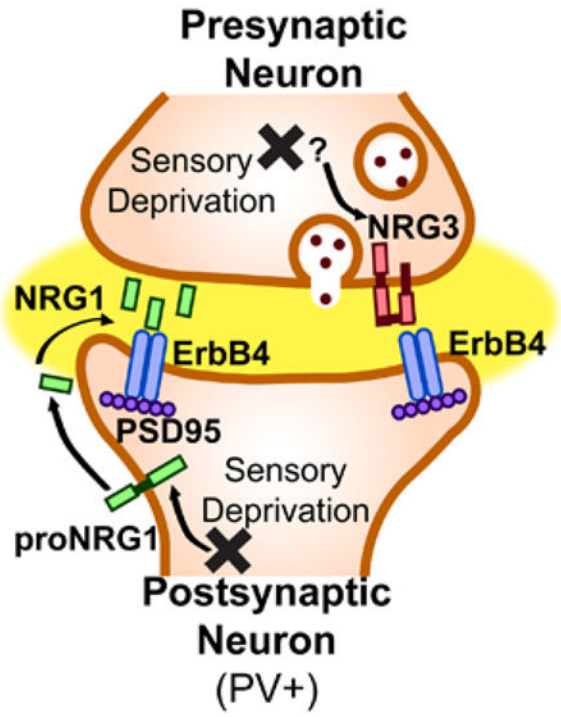

There are several neuregulins and ErbBs that may contribute to, visual cortical plasticity during the 'critical period' or during adulthood. Herein, it is determined that sensory deprivation results in downregulation of *nrg1* expression in PV, cells and results in changes in *nrg3* expression in way that depends on the type of deprivation.

Keywords

NRG1; ErbB4; parvalbumin; visual cortex; sensory deprivation; plasticity; RRID:AB_10000345; RRID:AB_477652; RRID:AB_634551

1. Introduction

Neural circuit plasticity is a feature of learning, memory and many other cognitive processes. During developmental "critical periods", neural circuitry can be profoundly shaped by sensory experience (Hensch, 2005). The critical period for visual cortical plasticity is a time restricted developmental window when ocular dominance is highly plastic to sensory input (Hubel and Wiesel, 1970). During the critical period in mice (P18-P32), just brief monocular deprivation can induce ocular dominance plasticity (Gordon and Stryker, 1996). Dark rearing animals can prolong the critical period (Fagiolini et al., 1994; Hensch, 2004). Further, adult plasticity beyond the critical period in the visual cortex can be reactivated by dark exposure (Hensch and Quinlan, 2018). Monocular deprivation, dark rearing and dark exposure are robust experimental manipulations that modulate critical visual cortical plasticity.

Neuregulins are a family of EGF domain-containing receptor ligands that are expressed in the nervous system, among which Neuregulin1 (NRG1) is best characterized. It was recently discovered that NRG1/ErbB4 signaling in PV inhibitory interneurons is critical for the initiation of visual cortical plasticity by controlling excitatory synaptic inputs onto PV neurons and thus PV cell mediated cortical disinhibition that occurs following visual deprivation (Grieco et al., 2019; Gu et al., 2016; Sun et al., 2016). However, there are multiple types of NRGs and ErbBs known to be involved in the development and function of the nervous system. Some may potentially have differential contributions to visual cortical plasticity.

NRG3 is expressed very strongly throughout the cortex during development and adulthood (Anton et al., 2004; Bartolini et al., 2017; Li et al., 2012; Longart et al., 2004; Loos et al., 2014; Rahman et al., 2019; Zhang et al., 1997). Alternatively, NRG2 and NRG4 are present in adult cortex, but not at very high levels (Anton et al., 2004; Longart et al., 2004; Paramo et al., 2018; Yan et al., 2018). NRG3 is a ligand for ErbB4 but has a lower affinity for ErbB4 than does NRG1 (Hobbs et al., 2002; Jones et al., 1999; Zhang et al., 1997). Both NRG2 and NRG4 are ligands for the ErbB4 receptor, but their relative affinities *in vivo* are unclear (Carraway et al., 1997; Harari et al., 1999). NRG3 is thought to be expressed presynaptically from excitatory neuron axons that synapse onto ErbB4 expressing dendrites of PV interneurons in order to stabilize the synapse (Bartolini et al., 2017; Muller et al., 2018; Rahman et al., 2019; Vullhorst et al., 2017). Supporting this interaction are the findings that both NRG3 and ErbB4 mutant mice have increased gamma oscillations (Del Pino et al., 2013; Muller et al., 2018). NRG2 is thought to accumulate postsynaptically on the proximal dendrites of ErbB4 expressing dendrites of PV interneurons to act in an autocrine manner (Lee et al., 2015; Vullhorst et al., 2017; Vullhorst et al., 2015). As NRGs have multiple sources and express as membrane-bound versus cleaved extracellular pools, it is of interest to determine how these different sources regulate visual plasticity.

Therefore, to further understand the implications of NRG/ErbB in visual cortical plasticity, we have performed a detailed analysis of *nrg1,2,3,4* and *erbB1,2,3,4* mRNA expression from PV inhibitory neurons and excitatory neurons in the visual cortex at the critical period age (P28), younger adult age (P56) and older adult age (P104). Using the translating ribosome affinity purification (TRAP) strategy, translating polyribosomes (polysomes) from specific cell types are tagged and then captured and used for purification of PV- or Excitatory-specific mRNAs (Zhou et al., 2013). We cross PV-Cre mice to fsTRAP mice to facilitate PV neuron specific mRNA expression analysis, and we cross EMX1-Cre mice to fsTRAP mice to facilitate excitatory neuron specific mRNA expression analysis (Gorski et al., 2002; Hippenmeyer et al., 2005; Sun et al., 2016). To test the effects of changes in sensory input that alter developmental and physiological outcomes during and after the critical period of visual cortical plasticity, we compared *nrg1,2,3,4* and *erbB1,2,3,4* mRNA expression in visual cortex in normal versus monocularly deprived mice at P28; normal versus dark reared mice at P28; and normal versus dark exposed adult mice at P104. Our data provide new important information of the cell specific expression of *nrg1,2,3,4* and *erbB1,2,3,4* mRNA in visual cortex development and their functional relevance to the regulation of critical period and adult cortical plasticity.

2. Materials and Methods

Animals

All experimental procedures and protocols were approved by the Institutional Animal Care and Use Committee of the University of California, Irvine. To enable PV-specific labeling and mRNA expression analysis, PV-ires-Cre mice (Jackson Laboratory, stock #017320) were crossed to fsTRAP mice (Zhou et al., 2013)(Jackson Laboratory, stock #022367) to generate PV-Cre+/−; fsTRAP mice, in which translating polyribosomes of PV cells are tagged with EGFP from the GFP-L10 transgene. To enable excitatory neuron labeling and mRNA expression analysis, Emx1-Cre mice (Jackson Laboratory, stock #005628) were crossed to fsTRAP mice to generate Emx1-Cre+/−; fsTRAP mice. EMX1 is predominantly expressed in cortical excitatory neurons with some expression in glial cells (Gorski et al., 2002). For all experiments mice were hemizygous for both transgenes. The animals (2–5 mice per cage) were housed in a vivarium room with a 12-h light/dark cycle (except for sensory deprivation experiments) with access to food and water ad libitum.

Mice were randomly assigned to either control or sensory deprivation groups. For monocular deprivation (MD) experiments (Kuhlman et al., 2013; Sun et al., 2016), at P27 one eye was sutured shut. One day later at P28, the contralateral V1 was harvested for mRNA extraction. For dark experiments sensory deprivation was performed in a vivarium room on a 24-h dark cycle within which mice were kept in a light-tight (0 Lux) ventilated box. For the dark rearing experiments, at P5 mice either continued developing under normal 12-h light/dark cycle conditions, or were housed in complete darkness until P28 (Gianfranceschi et al., 2003; Iwai et al., 2003). At P28 control and dark reared mice were sacrificed and V1 tissue was harvested for mRNA extraction. For dark exposure experiments, at P90 mice either continued aging under normal 12-h light/dark cycle conditions, or were housed in complete darkness until P104 (Erchova et al., 2017; Murase et al., 2017; Stodieck et al., 2014). At P104 control and dark exposed mice were sacrificed and V1 tissue was harvested for mRNA extraction. For PV-Cre; fsTRAP experiments, both cortices (V1) (except for MD experiments where only contralateral V1 was harvested from 10 miced to generate an n=1) from 5 mice were pooled together to generate each sample before mRNA extraction. For Emx1-Cre; fsTRAP experiments both cortices (V1) (except for MD experiments where only contralateral V1 was harvested) from 2 mice were pooled for each sample before mRNA extraction. ~350 fsTRAP mice were used to complete these studies.

Immunohistochemistry

For immunochemical staining experiments, animals were first deeply anesthetized with Uthasol (sodium pentobarbital, 100 mg/kg, i.p.) and were then perfused transcardially with 5mL of 1X phosphate buffered saline (PBS, pH 7.3–7.4), followed by 20 mL 1X PBS containing 4% paraformaldehyde (PFA) and phosphatase inhibitor (PhosSTOP, 1 tablet for 20 ml, Roche, Switzerland). Brains were removed and maintained in 4% PFA for 24 hours, and then transferred to 30% sucrose in 1X PBS for 24 hours. Then, using a freezing microtome (Leica SM2010R, Germany), coronal sections of the brain were taken at a 30 uM thickness. Mouse V1 coronal sections from bregma −3.40 to −3.80 mm were used for immunohistochemical staining and analysis.

Free floating sections were rinsed 5 times with 1X PBS, and incubated in a blocking solution for 1 hour at room temperature on a shaker. The blocking solution contained 5% normal donkey serum and 0.25% Triton X in 1X PBS. Sections were then incubated with the primary antibody diluted in blocking solution for 36 hours at 4 °C (Sun et al., 2016; Xu et al., 2010). After incubation with the primary antibody, brain sections were rinsed thoroughly with 1X PBS, and then incubated with the secondary antibody diluted in blocking solution for 2 hours at room temperature. After the secondary antibody was rinsed off, sections were counterstained with 10 μM 4'−6-diamidino-2- phenylindole (DAPI; Sigma-Aldrich, St. Louis, MO) for 5 minutes to help distinguish cortical laminar structure and neuronal nuclei. Lastly, sections were rinsed and then mounted on microscope slides. Sections were cover-slipped with Vectashield mounting medium (H-1000, Vector, Burlingame, CA). To identify PV positive neurons in PV-Cre; fsTRAP mice, the primary goat anti-PV antibody (PVG-213, Swant, Switzerland; RRID:AB_10000345; 1:1000) and a Cy3-conjugated donkey anti-goat antibody (Jackson ImmunoResearch, 1:200) were used. To identify GABA positive neurons in Emx1-Cre; fsTRAP mice, the primary rabbit anti-GABA antibody (A2052, SigmaAldrich; RRID:AB_477652; 1:1000) and a Cy3-conjugated donkey anti-rabbit antibody (Jackson ImmunoResearch, 1:200) were used. To identify CamkIIa positive neurons in Emx1-Cre; fsTRAP mice, the primary rabbit anti-CamkIIa antibody (sc-9035, Santa Cruz; RRID:AB_634551; 1:1000) and a Cy3-conjugated donkey anti-rabbit antibody (Jackson ImmunoResearch, 1:200) were used.

Immunostained sections were examined, and 10X and 40X image stacks were acquired using a confocal microscope (LSM 780, Carl Zeiss Microscopy,Germany). Image tiles, overlaying, maximum projections, and subset z-stack selections were performed using the Zeiss image processing software. For fluorescent imaging, all sections of a staining series were acquired using the same settings (laser power, pinhole size, line scans), and data images were digitally processed identically.

Translating Ribosome Affinity Purification (TRAP)

Purification of polysomally bound mRNA from visual cortical lysate was performed as described with modifications (Zhou et al., 2013). Briefly, visual cortex was dissected in ice-cold ACSF (in mM: 126 NaCl, 2.5 KCl, 26 $NaHCO_3$, 2 $CaCl_2$, 2 $MgCl_2$, 1.25 NaH_2PO_4, and 10 glucose). Pooled visual cortex from two to five mice was grinded to powder on dry ice, followed with sonication for 5 seconds in ice-cold lysis buffer [20 mM HEPES (pH 7.4), 150 mM KCl, 5 mM $MgCl_2$, 0.5 mM dithiothreitol, 100 μg/ml cycloheximide (Sigma-Aldrich), protease inhibitors (Roche) and 40 U/mL recombinant RNase inhibitor (Promega, Madison, WI)]. Homogenates were centrifuged for 10 minutes at 2,000x g, 4 °C, to pellet nuclei and large cell debris, and NP40 (Invitrogen, Carlsbad, CA) and DHPC (Avanti Polar Lipids, Alabaster, Alabama) were added to the supernatant at final concentrations of 1% (vol/vol) and 30 mM, respectively. After incubation on ice for 5 minutes, the lysate was centrifuged for 10 minutes at 20,000x g to pellet insoluble material. Two mouse monoclonal anti-GFP antibodies, Htz-GFP19C8 and Htz-GFP19F7 (50 μg each, Memorial Sloan-Kettering Monoclonal Antibody Facility, New York, NY) were added to bind to 375 μL protein G Dynal magnetic beads (Invitrogen). Alternatively, 300 μL of the streptavidin Myone T1 dynabeads were binding to 120 μL 1 μg/μL biotinylated protein L first, then

followed with two mouse monoclonal anti-GFP antibodies incubation. After being washed twice with the polysome extraction buffer, the beads were then added to the cell lysate supernatant, and the mixture was incubated at 4 °C with end over end rotation for 30 minutes. The beads were subsequently collected on a magnetic rack and washed four times with high salt polysome wash buffer [20 mM HEPES (pH 7.4), 350 mM KCl, 5 mM $MgCl_2$, 1% NP-40, 0.5 mM dithiothreitol and 100 μg/mL cycloheximide]. RNA was eluted from the beads by incubating beads in RLT buffer (Rneasy Micro Kit, Qiagen, Venlo, Netherlands) with β-mercaptoethanol (10 μL/mL) for 5 minutes at room temperature. Eluted RNA was purified using RNeasy Micro Kit (Qiagen) per the manufacturer's instructions including in-column DNase digestion. Immunoprecipitated RNA yield for each sample was approximately 20 ng/μL.

Quantitative Real-Time Polymerse Chain Reaction (qPCR)

Purified RNA (30ng) was converted to cDNA using Superscript® III reverse transcriptase (Thermo Fisher Scientific, Waltham, MA, USA) according to the manufacturer's instructions. Quantitative changes in cDNA levels were determined by real-time PCR using the Power SYBR Green Master Mix (Thermo Fisher Scientific, Waltham, MA, USA), using primers at a concentration of 500nM. Primers were for mouse *nrg1–4*, *erbB1–4*, and for the endogenous control *gapdh*. PCR was carried out for 2 min 50 °C, 5 min 95 °C, 40 cycles (15 seconds for 95°C, 30 seconds for 50°C), followed by a melt curve. Technical triplicates were used. All results were analyzed using the ddCt method with *gapdh* as an endogenous control, along with normalization to PV P28 *nrg1* expression, as indicated by a horizontal mark y-axis, so that all panels (b, c, d and e) within each figure could be compared (Livak and Schmittgen, 2001). Cycling and quantitation were performed on a ViiA™ 7 Real-Time PCR System instrument (Thermo Fisher Scientific, Waltham, MA, USA) using the ViiA 7 software v1.2. The following primers were used: NRG1-F GCAAGTGCCCAAATGAGTTTAC; NRG1-R GCTCCTCCGCTTCCATAAAT; NRG2-F GAGAGGTGGGTGAGAAGCAG; NRG2-R CGAATATCACGACTCCGGTT; NRG3-F GCATCCAGCACAAAGTCTGA; NRG3-R GTGCTTGATAGGCTGGCTTC; NRG4-F CAGACCAAGAGTCCAGCACA; NRG4-R AATACCAGTTTCCGCACAGG; ErbB1-F GCTGGTGTTGCTGACCGCG; ErbB1-R GGGTGAGCCTGTTACTTGTGCC; ErbB2-F GCAAGCACTGTCTGCCATGC; ErbB2-R GGGCACAAGCCTCACACTGG; ErbB3-F CGAGATGGGCAACTCTCAGGC; ErbB3-R AGGTTACCCATGACCACCTCACAC; ErbB4-F CATGGCCTTCCAACATGACTCTGG; ErbB4-R GGCAGTGATTTTCTGTGGGTCCC; GAPDH-F TGCCAACATCACCATTGTTGA; GAPDH-R TGCCAACATCACCATTGTTGA.

Statistical Analysis

All data are reported as mean ± SEM. When comparing two independent groups, normally distributed data were analyzed using a Student's t test. In the case data were not normally distributed, a Mann-Whitney U test was used. In the case more than two groups were compared and data were normally distributed, an ANOVA was performed and followed by post hoc comparisons when justified. In other cases, a non-parametric one-way ANOVA Kruskal Wallis test was used and followed by comparisons with Mann-Whitney U tests. A p value (%0.05) was considered statistically significant.

For TRAP experiments sample size n was defined as n=1 for PV-Cre; fsTRAP when both V1 cortices from 5 animals were pooled. For Emx1-Cre; fsTRAP an n=1 was defined as both V1 cortices from 2 animals pooled together. In the case of quantitative immunochemical analysis 'n' was defined as cell or group number.

Results

Characterization of PV-Cre; fsTRAP and Emx1-Cre; fsTRAP Mice

In order to determine how the expression of *nrg1,2,3,4* and *erbB1,2,3,4* mRNA by PV or excitatory cells is modulated following visual deprivation, we determined their gene expression in a cell specific manner using the translating ribosome affinity purification (TRAP) strategy (Zhou et al., 2013). fsTRAP mice were crossed with mice that either express Cre recombinase with PV inhibitory cell specificity (PV-Cre; fsTRAP, (Hippenmeyer et al., 2005), or with excitatory neuron cell specificity (Emx1-Cre; fsTRAP, (Gorski et al., 2002). This strategy allows for the isolation of cell specific mRNAs bound to translating ribosomes tagged with EGFP (Figure 1a). In PV-Cre; fsTRAP mice, the fsTRAP-EGFP transgene is expressed in a PV cell specific manner at P28 (Figure 1b). Nearly all genetically labeled PV cells are strongly immunopositive for PV, reciprocally, no PV immunopositive cells lack genetic labeling (Figure 1c,f,g). In Emx1-Cre; fsTRAP mice, the fsTRAP-EGFP transgene expression is excluded from inhibitory neurons, and colocalized with excitatory neurons, as nearly none of the genetically labeled Emx1+ cells are immunopositive for GABA at P28 (Figure 1d,f,h), and almost all are immunopositive for CamkIIa (Figure 1e,f,i). Therefore, the PV-Cre; fsTRAP and Emx1-Cre; fsTRAP mice were used for subsequent experimentation.

Normal NRG and ErbB Expression in PV Inhibitory Interneurons and Excitatory Neurons through the Critical Period and into Adulthood

Although NRG1/ErbB4 has been implicated in visual cortical plasticity, NRG/ErbB signaling has significant crosstalk (Mei and Nave, 2014). To map temporal expression of this signaling family, we measured the expression of *nrg1,2,3,4* and *erbB1,2,3,4* mRNA by PV or excitatory cells in visual cortex using qPCR during the critical period and into adulthood (Figure 2a). Results are relative to P28 PV cell specific *nrg1* expression for each Figure, as indicated by a horizontal tick mark on the y-axis, allowing for comparisons between panels within each Figure. For example expression levels in Figure 2b,c,d and e can be compared.

We find that *nrg1* expression in PV interneurons decreases after peak expression during the critical period from P28 to P104 (Figure 2b). Between p28 to p56, *nrg1* shows a 76% reduction in expression, and between P28 to P104, it remains lower at a 56% reduction in expression (Figure 2b). In contrast, *nrg3* expression by PV interneurons increases significantly by 109% from P28 to P104, and by this assay appears to show higher expression than *nrg1* (Figure 2b). NRG3 also signals through the ErbB4 receptor, but the nature of this adult NRG3/ErbB4 signaling is not well understood, and NRG3 has a much lower affinity for ErbB4 than NRG1 (Hobbs et al., 2002; Jones et al., 1999; Zhang et al., 1997), which could differentially influence signaling. NRG3 has been reported to be expressed by inhibitory and PV interneurons (Muller et al., 2018; Rahman et al., 2019).

Neither *nrg2* nor *nrg4* expression by PV cells is strong, and do not change between P28 to P104 (Figure 2b).

While PV interneurons in the visual cortex express ErbB4 at high levels (Grieco et al., 2019; Gu et al., 2016; Sun et al., 2016), expression of the other ErbBs should be examined also. To test if ErbB4 forms heterodimers with other ErbBs allowing for NRG signaling (Mei and Nave, 2014) in PV neurons, the expression of four *erbB* family members were measured at P28, P56 and P104. PV cells express *erbB4* at very high levels compared to excitatory neurons, as described in previous reports, and thus validated the specificity of fsTRAP expression. *erbB4* is expressed at levels ~50 fold higher than the other ErbBs in PV or excitatory neurons (Figure 2c,e). Note that some expression of *erbBs* (in particular *erbB4*) in Emx1-Cre; fsTRAP may result from Emx1-expressing glial cells as Emx1-lineage cells contain cortical excitatory neurons and some glia (but not GABAergic neurons) (Gorski et al., 2002).

Although NRG1 immunoreactivity in visual cortex is detected in excitatory cells in the mouse visual cortex, it is still unclear whether excitatory neurons express other NRGs, since they are transmembrane proteins that are cleaved prior to extracellular binding of ErbBs, and are thus capable of diffusion post cleavage (Mei and Nave, 2014; Vullhorst et al., 2017). We measured age-dependent *nrg1,2,3,4* mRNA expression by qPCR in excitatory neurons. The expression of *nrg3* increases by 72% in excitatory neurons from P28 to P104, similar to the age-dependent increase in *nrg3* expression in PV neurons, and *nrg3* is expressed at higher levels than the other NRGs in excitatory neurons (Figure 2d). In contrast, no significant changes with age are observed for *nrg1,2 or 4* (Figure 2d), which suggests potential adult specific roles for NRG3.

Since NRGs signal through the ErbBs, we determined age-dependent *erbB1,2,3,4* mRNA expression in excitatory neurons. Both *erbB1* and *erbB3* expression, show significant age-related reductions in excitatory neurons (Figure 2e). The expression of *erbB1* is reduced by 74% between P28 to P104 (Figure 2e). The expression of *erbB3* shows monotonic age-related reduction, with expression reduced by 69% between P28 to P56 and by 89% between P28 to P104. The expression of *erbB2* and *erbB4* remain relatively low and unchanged with age (Figure 2e). Of the ErbBs, both ErbB3 and ErbB4 bind the NRGs as homodimers, but ErbB1 and ErbB2 can also form heterodimers with ErbB3 or ErbB4 (Riese et al., 1995). ErbB2 functions mainly as a heterodimer forming partner for the other ErbBs (Graus-Porta et al., 1997). Expression of all the ErbBs has been reported in the cortex through development and into adulthood, and there is some evidence supporting that ErbB1 and ErbB3 levels may drop in adulthood (Fox and Kornblum, 2005). These findings reveal the cell specific regulation of *nrg1,2,3,4*, particularly *nrg1* and *nrg3*, and *erbB* expression, in visual cortex during development and into adulthood (Figure 2, Table 1a,b,c).

NRG and ErbB Expression by PV and Excitatory Neurons after Monocular Deprivation during the Developmental Critical Period

Considering the possibility that NRG/ErbB signaling may exhibit cell specific plastic changes in expression following sensory deprivation, we measured the expression of *nrg1,2,3,4* and *erbB1,2,3,4* mRNA by qPCR during the critical period in PV and excitatory

neurons in contralateral visual cortex after 1 day of monocular deprivation (MD)(Figure 3a). Brief MD during the critical period can induce aspects of visual cortical plasticity (Espinosa and Stryker, 2012). In fact, MD for only 1 day can significantly reduce the activity of PV interneurons, and reduce PV NRG1/ErbB4 signaling (Kuhlman et al., 2013; Sun et al., 2016). For controls, we compared expression from the left cortices (right eyes were sutured in the MD group) of age-matched non-deprived animals co-processed at the same times (Figure 3a).

Nrg1 expression in PV visual cortical neurons drops significantly by 54% after monocular deprivation for 1 day (P27-P28) relative to non-deprived animals (Figure 3b). These results are in qualitative agreement with earlier findings of reduced *nrg1* expression by PV cells after monocular deprivation (Sun et al., 2016). Strikingly, there is also an acute 65% reduction in *nrg3* expression in PV cells immediately following monocular deprivation (Figure 3b). The expression of *erbB1,2,3* are significantly upregulated in PV neurons after monocular deprivation, although they express at very low levels compared to *erbB4*, which remains stable and unchanged following monocular deprivation (Figure 3c).

In excitatory cells, monocular deprivation also decreases *nrg3* expression significantly by 45% compared to normal animals (Figure 3d). In contrast, no other changes in expression of the other *nrgs* or *erbBs* are observed in excitatory neurons following acute monocular deprivation (Figure 3d–e).

NRG and ErbB Expression by PV and Excitatory Neurons after Dark Rearing during the Developmental Critical Period

Deprivation of visual sensory experience by dark rearing (DR) animals can postpone closure of the critical period (Fagiolini et al., 1994; Gianfranceschi et al., 2003; Hensch, 2004; Iwai et al., 2003). To test changes in the expression of *nrg1,2,3,4* and *erbB1,2,3,4* mRNA associated with critical period regulation and potential plasticity evoked by dark rearing, we measured expression of these genes in PV versus excitatory neurons in visual cortex using qPCR following normal versus dark rearing in critical period aged animals at P28 (Figure 4a).

After dark rearing animals to an age (P28), an age that approaches the closure of the critical period (~P32), *nrg1* expression by PV cells in visual cortex drops significantly by 83% (Figure 4b) in dark reared mice compared to normally reared mice. Peak expression of NRG1 on PV cells was previously found to occur at ~P28 after normal rearing – this peak appears to signal the onset of the critical period closure (Sun et al., 2016). Thus, decreased *nrg1* expression after dark rearing may functionally reflect a delay of the critical period closure that extends visual cortical plasticity to later ages. Dark rearing also evokes a 35% reduction in *nrg3* expression in PV neurons (Figure 4b). In contrast to dark rearing evoked changes in *nrg1* and *nrg3* mRNAs, there are no other significant changes for any of the other *nrgs* or *erbBs* mRNAs for PV or excitatory cells after dark rearing (Figure 4b–e). *nrg2* and *nrg4* mRNA expression in PV neurons remain low following either normal or dark rearing (Figure 4b); and *erbB1,2,3* expression in PV neurons remain low following either normal or dark rearing (Figure 4c). *erbB4* mRNA expression in PV neurons remains consistently high following either normal or dark rearing (Figure 4c). The reduction in *nrg1* and *nrg3*

expression by PV cells after dark rearing may represent the early critical period conditions when NRG1 levels are still low, before approaching the closure of the critical period for visual cortical plasticity (Grieco et al., 2019; Sun et al., 2016).

NRG and ErbB Expression by PV and Excitatory Neurons after Dark Exposure during Adulthood

As noted above, although the critical period is normally confined to postnatal development, dark exposure during adulthood can reset aspects of adult visual cortex to what is observed with juveniles during the critical period (He et al., 2007; Hensch and Quinlan, 2018). To test changes in the expression of *nrg1,2,3,4* and *erbB1,2,3,4* mRNA in response to dark exposure, we measured mRNA expression of these genes using qPCR after 2 weeks of dark exposure in adult animals in PV versus excitatory cells in visual cortex (Figure 5a)(Erchova et al., 2017; Murase et al., 2017; Stodieck et al., 2014). After dark exposing adult animals for 2 weeks (P90-P104), *nrg1* mRNA expression from visual cortical PV neurons drops significantly by 63% in dark exposed animals compared to normal animals (Figure 5b). This suggests that adult dark exposures can evoke PV neuron *nrg1* mRNA expression changes similar to juvenile visual cortex during deprivation induced ocular dominance plasticity during the critical period.

Nrg3 mRNA expression by PV cells in visual cortex is significantly reduced by 53% following adult dark exposure compared to normal animals (Figure 5b). In contrast, adult dark exposures significantly increases *nrg3* mRNA expression in excitatory cells by 65% compared to normal animals (Figure 5d). No other adult dark exposure changes in mRNA expression of the other *nrgs* or *erbBs* are observed in either PV or excitatory neurons (Figure 5b–e).

Discussion

Although we and others found that NRG1/ErbB4 signaling by PV interneurons regulates visual cortical ocular dominance plasticity (Grieco et al., 2019; Gu et al., 2016; Sun et al., 2016), the present work addresses outstanding questions about the details of NRG1/ErbB4 signaling by PV interneurons and excitatory neurons and their involvement in critical period and adult cortical plasticity (Figure 6a–b). Since NRG1 immunoreactivity on PV and excitatory neurons drops significantly following the critical period, and ErbB4 expression by PV neurons remains high into adulthood, it is unclear what ErbB4 ligand is functionally important for adult plasticity. We find that although *nrg1* mRNA expression normally drops after the critical period in PV cells but not excitatory neurons, *nrg1* mRNA expression still retains the dynamic capacity to be downregulated in PV neurons with adult sensory manipulations (dark exposure) that induce adult cortical plasticity (Figure 6c–e). This suggests that NRG1 may have the potential to act via PV ErbB4 in regulating visual cortical plasticity during adulthood.

The cellular source of functional NRG1 is still unclear. Since NRG1 is cleaved extracellularly, allowing for its release and diffusion in the extracellular space, localizing NRG1's cellular source using immunochemical methods is difficult (Vullhorst et al., 2017). Using immunostaining, Sun et al., 2016 determined that NRG1 immunoreactivity is present

at roughly equal levels in PV interneurons and excitatory neurons. Using the TRAP technique, *nrg1* mRNA is more abundant in PV cells than excitatory neurons. With monocular deprivation during the critical period, NRG1 immunoreactivity in PV neurons decreases but remains unchanged in excitatory neurons. Consistently, *nrg1* mRNA decreases in PV neurons after monocular deprivation, but *nrg1* mRNA changes in excitatory neurons was not reported (Sun et al., 2016). In the present study, we determined that during the critical period, monocular deprivation evokes decreased *nrg1* mRNA expression in PV but not in excitatory neurons. In addition, sensory deprivation during the critical period by dark rearing mice also reduces *nrg1* mRNA expression in PV cells but not in excitatory neurons. Therefore, changes in NRG1 immunoreactivity in PV neurons evoked by sensory deprivation are likely consistent with reductions in PV neuron *nrg1* mRNA expression. These findings provide support for the hypothesis that NRG1/ErbB4 signaling in PV interneurons is regulated in an autocrine fashion and is modulated by sensory input.

One intriguing question raised by these findings are the results that both during the critical period and adulthood, sensory deprivation induces reductions in *nrg1* expression by PV neurons (Figure 6c–e). The timing of *nrg1* expression downregulation by PV neurons coinciding with ages past the normal timing of the closing of the visual critical period is also very interesting. These observations support two levels of control of a single mechanism. One potential explanation is that with changes in visual cortical activity during sensory deprivation, PV *nrg1* expression is reduced in a joint activity-dependent and cell-autonomous feedback mechanism (Eilam et al., 1998; Ozaki et al., 2004). On a larger scale, the PV *nrg1* expression apex during the critical period and subsequent reduction is also supported by a joint activity-dependent and cell-autonomous feedback mechanism. Increased PV *nrg1* expression may be driven by activity in the visual cortex during synaptic competition in the critical period. After cortical inhibition is established with the closure of the critical period PV *nrg1* expression may then decrease, similar to the response to sensory deprivation. Since PV *nrg1* expression after the critical period is reduced, this suggests that post-critical period activity changes in the circuits surrounding PV neurons trigger PV *nrg1* baseline expression to move to a new reduced level (Figure 6e). The maturation of visual ocular dominance may itself be the trigger for the developmental decrease in *nrg1* as changes in excitatory-inhibitory balance influence NRG1's optimum levels (Agarwal et al., 2014).

NRG3 is a paralog of NRG1 and binds ErbB4 (Zhang et al., 1997). However, NRG3 has a lower affinity for ErbB4 than does NRG1 (Hobbs et al., 2002; Jones et al., 1999). Importantly, expression of *nrg1* and *nrg3* diverge with aging. While *nrg1* expression decreases with age, *nrg3* expression increases after the critical period (Figure 6e). NRG3 interacts with the ErbB4 receptor by juxtacrine signaling from excitatory neuron axons (Vullhorst et al., 2017). Therefore, *nrg3* expression from excitatory neurons may functionally complement reductions in NRG1 signaling, by maintaining excitatory inputs to PV neurons, as animals age past the critical period. The situation is complicated by variable changes in *nrg3 expression* patterns from excitatory neurons that depend on what type of sensory deprivation is experienced. Whereas *nrg1* expression from PV neurons is consistently reduced with deprivation, *nrg3* expression changes with excitatory neurons, depends heavily on the type of sensory deprivation (Figure 6c–e) However, unlike *nrg1* and

nrg3 expression, neither *nrg2* nor *nrg4* expression are modulated with age and or by juvenile or adult sensory deprivation. While this does not exclude them from potential roles in sensory cortical development or plasticity, their relative lack of change suggests that they have lesser priority for future investigations.

Though *nrg1* and *nrg3* expression is heavily modulated with age and sensory deprivation, the expression of their receptor, *erbB4*, is unchanged. In the brain, ErbB4 is the most abundant of all ErbBs, and represents the major receptor for NRGs (Bernstein et al., 2006; Fox and Kornblum, 2005; Gerecke et al., 2001; Neddens and Buonanno, 2011; Steiner et al., 1999). ErbB4 is primarily expressed by PV interneurons at their dendrites (Chen et al., 2010; Fazzari et al., 2010; Lu et al., 2014; Neddens and Buonanno, 2010; Tan et al., 2011; Vullhorst et al., 2009; Wen et al., 2010; Yau et al., 2003). Robust *erbB4* expression by PV cells across different ages and sensory manipulations suggests, 1) maintaining ErbB4 signaling is important for PV neurons, and 2) the modulation of ErbB4 signaling is mostly done at the level of the ligand (Figure 6 c–d). In addition, since *erbB4* expression in PV neurons is very high compared to *erbB1–3* expression, it is likely that ErbB4 signaling by PV interneurons is mostly done through ErbB4 homodimer binding of ligands. The expression of *erbB1* and *erbB3* do show age related developmental decreases in excitatory neurons, making them potential candidates for further physiological investigation.

nrg1 expression by PV interneurons is reduced by visual deprivation, either during or after the critical period. This response may function to weaken excitatory inputs to PV inhibitory interneurons, thus increasing visual cortical responsiveness to stimulate cortical plasticity (Figure 6b). However, after the closure of the visual critical period, *nrg1* expression by PV interneurons is reduced, suggesting that this visual cortical niche of PV cells under normal sensory conditions changes. Interestingly, after the critical period, *nrg3* expression increases in excitatory neurons. Since NRG3 can signal through ErbB4 by juxtacrine interactions (Figure 6 c–d), and is likely the most abundant NRG in visual cortex, increases in *nrg3* expression by excitatory neurons could drive reductions in PV *nrg1* expression. However, the functional role of PV expressed NRG3 is unclear, thus it is not included in the model proposed in Figure 6. Given the potential interplay/cooperation of NRG1 and NRG3 in controlling visual cortex development and plasticity, future studies will need to address this relationship, potentially by using cell type specific NRG1 or NRG3 overexpression or ablation. These findings could elucidate the underlying causal relationship between NRG1 and NRG3 cell type specific expression, and the mechanisms differentiating critical period versus adult visual cortical plasticity.

Acknowledgements

This work was supported by US National Institutes of Health (NIH) grants R01EY028212, R01EY027407 and R01 MH105427 (X.X). TCH is supported by NIH grant R35 GM127102.

References

Agarwal A, Zhang M, Trembak-Duff I, Unterbarnscheidt T, Radyushkin K, Dibaj P, Martins de Souza D, Boretius S, Brzozka MM, Steffens H, et al. (2014). Dysregulated expression of neuregulin-1 by cortical pyramidal neurons disrupts synaptic plasticity. Cell Rep 8, 1130–1145. [PubMed: 25131210]

Anton ES, Ghashghaei HT, Weber JL, McCann C, Fischer TM, Cheung ID, Gassmann M, Messing A, Klein R, Schwab MH, et al. (2004). Receptor tyrosine kinase ErbB4 modulates neuroblast migration and placement in the adult forebrain. Nat Neurosci 7, 1319–1328. [PubMed: 15543145]

Bartolini G, Sanchez-Alcaniz JA, Osorio C, Valiente M, Garcia-Frigola C, and Marin O (2017). Neuregulin 3 Mediates Cortical Plate Invasion and Laminar Allocation of GABAergic Interneurons. Cell Rep 18, 1157–1170. [PubMed: 28147272]

Bernstein HG, Lendeckel U, Bertram I, Bukowska A, Kanakis D, Dobrowolny H, Stauch R, Krell D, Mawrin C, Budinger E, et al. (2006). Localization of neuregulin-1alpha (heregulin-alpha) and one of its receptors, ErbB-4 tyrosine kinase, in developing and adult human brain. Brain Res Bull 69, 546–559. [PubMed: 16647583]

Carraway KL 3rd, Weber JL, Unger MJ, Ledesma J, Yu N, Gassmann M, and Lai C (1997). Neuregulin-2, a new ligand of ErbB3/ErbB4-receptor tyrosine kinases. Nature 387, 512–516. [PubMed: 9168115]

Chen YJ, Zhang M, Yin DM, Wen L, Ting A, Wang P, Lu YS, Zhu XH, Li SJ, Wu CY, et al. (2010). ErbB4 in parvalbumin-positive interneurons is critical for neuregulin 1 regulation of long-term potentiation. Proc Natl Acad Sci U S A 107, 21818–21823. [PubMed: 21106764]

Del Pino I, Garcia-Frigola C, Dehorter N, Brotons-Mas JR, Alvarez-Salvado E, Martinez de Lagran M, Ciceri G, Gabaldon MV, Moratal D, Dierssen M, et al. (2013). Erbb4 deletion from fast-spiking interneurons causes schizophrenia-like phenotypes. Neuron 79, 1152–1168. [PubMed: 24050403]

Eilam R, Pinkas-Kramarski R, Ratzkin BJ, Segal M, and Yarden Y (1998). Activity-dependent regulation of Neu differentiation factor/neuregulin expression in rat brain. Proc Natl Acad Sci U S A 95, 1888–1893. [PubMed: 9465112]

Erchova I, Vasalauskaite A, Longo V, and Sengpiel F (2017). Enhancement of visual cortex plasticity by dark exposure. Philos Trans R Soc Lond B Biol Sci 372.

Espinosa JS, and Stryker MP (2012). Development and plasticity of the primary visual cortex. Neuron 75, 230–249. [PubMed: 22841309]

Fagiolini M, Pizzorusso T, Berardi N, Domenici L, and Maffei L (1994). Functional postnatal development of the rat primary visual cortex and the role of visual experience: dark rearing and monocular deprivation. Vision Res 34, 709–720. [PubMed: 8160387]

Fazzari P, Paternain AV, Valiente M, Pla R, Lujan R, Lloyd K, Lerma J, Marin O, and Rico B (2010). Control of cortical GABA circuitry development by Nrg1 and ErbB4 signalling. Nature 464, 1376–1380. [PubMed: 20393464]

Fox IJ, and Kornblum HI (2005). Developmental profile of ErbB receptors in murine central nervous system: implications for functional interactions. J Neurosci Res 79, 584–597. [PubMed: 15682390]

Gerecke KM, Wyss JM, Karavanova I, Buonanno A, and Carroll SL (2001). ErbB transmembrane tyrosine kinase receptors are differentially expressed throughout the adult rat central nervous system. J Comp Neurol 433, 86–100. [PubMed: 11283951]

Gianfranceschi L, Siciliano R, Walls J, Morales B, Kirkwood A, Huang ZJ, Tonegawa S, and Maffei L (2003). Visual cortex is rescued from the effects of dark rearing by overexpression of BDNF. Proc Natl Acad Sci U S A 100, 12486–12491. [PubMed: 14514885]

Gordon JA, and Stryker MP (1996). Experience-dependent plasticity of binocular responses in the primary visual cortex of the mouse. J Neurosci 16, 3274–3286. [PubMed: 8627365]

Gorski JA, Talley T, Qiu M, Puelles L, Rubenstein JL, and Jones KR (2002). Cortical excitatory neurons and glia, but not GABAergic neurons, are produced in the Emx1-expressing lineage. J Neurosci 22, 6309–6314. [PubMed: 12151506]

Graus-Porta D, Beerli RR, Daly JM, and Hynes NE (1997). ErbB-2, the preferred heterodimerization partner of all ErbB receptors, is a mediator of lateral signaling. EMBO J 16, 1647–1655. [PubMed: 9130710]

Grieco SF, Holmes TC, and Xu X (2019). Neuregulin directed molecular mechanisms of visual cortical plasticity. J Comp Neurol 527, 668–678. [PubMed: 29464684]

Gu Y, Tran T, Murase S, Borrell A, Kirkwood A, and Quinlan EM (2016). Neuregulin-Dependent Regulation of Fast-Spiking Interneuron Excitability Controls the Timing of the Critical Period. J Neurosci 36, 10285–10295. [PubMed: 27707966]

Harari D, Tzahar E, Romano J, Shelly M, Pierce JH, Andrews GC, and Yarden Y (1999). Neuregulin-4: a novel growth factor that acts through the ErbB-4 receptor tyrosine kinase. Oncogene 18, 2681–2689. [PubMed: 10348342]

He HY, Ray B, Dennis K, and Quinlan EM (2007). Experience-dependent recovery of vision following chronic deprivation amblyopia. Nat Neurosci 10, 1134–1136. [PubMed: 17694050]

Hensch TK (2004). Critical period regulation. Annu Rev Neurosci 27, 549–579. [PubMed: 15217343]

Hensch TK (2005). Critical period plasticity in local cortical circuits. Nat Rev Neurosci 6, 877–888. [PubMed: 16261181]

Hensch TK, and Quinlan EM (2018). Critical periods in amblyopia. Vis Neurosci 35, E014. [PubMed: 29905116]

Hippenmeyer S, Vrieseling E, Sigrist M, Portmann T, Laengle C, Ladle DR, and Arber S (2005). A developmental switch in the response of DRG neurons to ETS transcription factor signaling. PLoS Biol 3, e159. [PubMed: 15836427]

Hobbs SS, Coffing SL, Le AT, Cameron EM, Williams EE, Andrew M, Blommel EN, Hammer RP, Chang H, and Riese DJ 2nd, (2002). Neuregulin isoforms exhibit distinct patterns of ErbB family receptor activation. Oncogene 21, 8442–8452. [PubMed: 12466964]

Hubel DH, and Wiesel TN (1970). The period of susceptibility to the physiological effects of unilateral eye closure in kittens. J Physiol 206, 419–436. [PubMed: 5498493]

Iwai Y, Fagiolini M, Obata K, and Hensch TK (2003). Rapid critical period induction by tonic inhibition in visual cortex. J Neurosci 23, 6695–6702. [PubMed: 12890762]

Jones JT, Akita RW, and Sliwkowski MX (1999). Binding specificities and affinities of egf domains for ErbB receptors. FEBS Lett 447, 227–231. [PubMed: 10214951]

Kuhlman SJ, Olivas ND, Tring E, Ikrar T, Xu X, and Trachtenberg JT (2013). A disinhibitory microcircuit initiates critical-period plasticity in the visual cortex. Nature 501, 543–546. [PubMed: 23975100]

Lee KH, Lee H, Yang CH, Ko JS, Park CH, Woo RS, Kim JY, Sun W, Kim JH, Ho WK, et al. (2015). Bidirectional Signaling of Neuregulin-2 Mediates Formation of GABAergic Synapses and Maturation of Glutamatergic Synapses in Newborn Granule Cells of Postnatal Hippocampus. J Neurosci 35, 16479–16493. [PubMed: 26674872]

Li H, Chou SJ, Hamasaki T, Perez-Garcia CG, and O'Leary DD (2012). Neuregulin repellent signaling via ErbB4 restricts GABAergic interneurons to migratory paths from ganglionic eminence to cortical destinations. Neural Dev 7, 10. [PubMed: 22376909]

Livak KJ, and Schmittgen TD (2001). Analysis of relative gene expression data using real-time quantitative PCR and the 2(-Delta Delta C(T)) Method. Methods 25, 402–408. [PubMed: 11846609]

Longart M, Liu Y, Karavanova I, and Buonanno A (2004). Neuregulin-2 is developmentally regulated and targeted to dendrites of central neurons. J Comp Neurol 472, 156–172. [PubMed: 15048684]

Loos M, Mueller T, Gouwenberg Y, Wijnands R, van der Loo RJ, Neuro BMPC, Birchmeier C, Smit AB, and Spijker S (2014). Neuregulin-3 in the mouse medial prefrontal cortex regulates impulsive action. Biol Psychiatry 76, 648–655. [PubMed: 24703509]

Lu Y, Sun XD, Hou FQ, Bi LL, Yin DM, Liu F, Chen YJ, Bean JC, Jiao HF, Liu X, et al. (2014).Maintenance of GABAergic activity by neuregulin 1-ErbB4 in amygdala for fear memory. Neuron 84, 835–846. [PubMed: 25451196]

Mei L, and Nave KA (2014). Neuregulin-ERBB signaling in the nervous system and neuropsychiatric diseases. Neuron 83, 27–49. [PubMed: 24991953]

Muller T, Braud S, Juttner R, Voigt BC, Paulick K, Sheean ME, Klisch C, Gueneykaya D, Rathjen FG, Geiger JR, et al. (2018). Neuregulin 3 promotes excitatory synapse formation on hippocampal interneurons. EMBO J 37.

Murase S, Lantz CL, and Quinlan EM (2017). Light reintroduction after dark exposure reactivates plasticity in adults via perisynaptic activation of MMP-9. Elife 6.

Neddens J, and Buonanno A (2010). Selective populations of hippocampal interneurons express ErbB4 and their number and distribution is altered in ErbB4 knockout mice. Hippocampus 20, 724–744. [PubMed: 19655320]

Neddens J, and Buonanno A (2011). Expression of the neuregulin receptor ErbB4 in the brain of the rhesus monkey (Macaca mulatta). PLoS One 6, e27337. [PubMed: 22087295]

Ozaki M, Itoh K, Miyakawa Y, Kishida H, and Hashikawa T (2004). Protein processing and releases of neuregulin-1 are regulated in an activity-dependent manner. J Neurochem 91, 176–188. [PubMed: 15379898]

Paramo B, Wyatt S, and Davies AM (2018). An essential role for neuregulin-4 in the growth and elaboration of developing neocortical pyramidal dendrites. Exp Neurol 302, 85–92. [PubMed: 29317193]

Rahman A, Weber J, Labin E, Lai C, and Prieto AL (2019). Developmental expression of Neuregulin-3 in the rat central nervous system. J Comp Neurol 527, 797–817. [PubMed: 30328115]

Riese DJ 2nd, van Raaij TM, Plowman GD, Andrews GC, and Stern DF (1995). The cellular response to neuregulins is governed by complex interactions of the erbB receptor family. Mol Cell Biol 15, 5770–5776. [PubMed: 7565730]

Steiner H, Blum M, Kitai ST, and Fedi P (1999). Differential expression of ErbB3 and ErbB4 neuregulin receptors in dopamine neurons and forebrain areas of the adult rat. Exp Neurol 159, 494–503. [PubMed: 10506520]

Stodieck SK, Greifzu F, Goetze B, Schmidt KF, and Lowel S (2014). Brief dark exposure restored ocular dominance plasticity in aging mice and after a cortical stroke. Exp Gerontol 60, 1–11. [PubMed: 25220148]

Sun Y, Ikrar T, Davis MF, Gong N, Zheng X, Luo ZD, Lai C, Mei L, Holmes TC, Gandhi SP, et al. (2016). Neuregulin-1/ErbB4 Signaling Regulates Visual Cortical Plasticity. Neuron 92, 160–173. [PubMed: 27641496]

Tan GH, Liu YY, Hu XL, Yin DM, Mei L, and Xiong ZQ (2011). Neuregulin 1 represses limbic epileptogenesis through ErbB4 in parvalbumin-expressing interneurons. Nat Neurosci 15, 258–266. [PubMed: 22158510]

Vullhorst D, Ahmad T, Karavanova I, Keating C, and Buonanno A (2017). Structural Similarities between Neuregulin 1–3 Isoforms Determine Their Subcellular Distribution and Signaling Mode in Central Neurons. J Neurosci 37, 5232–5249. [PubMed: 28432142]

Vullhorst D, Mitchell RM, Keating C, Roychowdhury S, Karavanova I, Tao-Cheng JH, and Buonanno A (2015). A negative feedback loop controls NMDA receptor function in cortical interneurons via neuregulin 2/ErbB4 signalling. Nat Commun 6, 7222. [PubMed: 26027736]

Vullhorst D, Neddens J, Karavanova I, Tricoire L, Petralia RS, McBain CJ, and Buonanno A (2009). Selective expression of ErbB4 in interneurons, but not pyramidal cells, of the rodent hippocampus. J Neurosci 29, 12255–12264. [PubMed: 19793984]

Wen L, Lu YS, Zhu XH, Li XM, Woo RS, Chen YJ, Yin DM, Lai C, Terry AV Jr., Vazdarjanova A, et al. (2010). Neuregulin 1 regulates pyramidal neuron activity via ErbB4 in parvalbumin-positive interneurons. Proc Natl Acad Sci U S A 107, 1211–1216. [PubMed: 20080551]

Xu X, Roby KD, and Callaway EM (2010). Immunochemical characterization of inhibitory mouse cortical neurons: three chemically distinct classes of inhibitory cells. J Comp Neurol 518, 389–404. [PubMed: 19950390]

Yan L, Shamir A, Skirzewski M, Leiva-Salcedo E, Kwon OB, Karavanova I, Paredes D, Malkesman O, Bailey KR, Vullhorst D, et al. (2018). Neuregulin-2 ablation results in dopamine dysregulation and severe behavioral phenotypes relevant to psychiatric disorders. Mol Psychiatry 23, 1233–1243. [PubMed: 28322273]

Yau HJ, Wang HF, Lai C, and Liu FC (2003). Neural development of the neuregulin receptor ErbB4 in the cerebral cortex and the hippocampus: preferential expression by interneurons tangentially migrating from the ganglionic eminences. Cereb Cortex 13, 252–264. [PubMed: 12571115]

Zhang D, Sliwkowski MX, Mark M, Frantz G, Akita R, Sun Y, Hillan K, Crowley C, Brush J, and Godowski PJ (1997). Neuregulin-3 (NRG3): a novel neural tissue-enriched protein that binds and activates ErbB4. Proc Natl Acad Sci U S A 94, 9562–9567. [PubMed: 9275162]

Zhou P, Zhang Y, Ma Q, Gu F, Day DS, He A, Zhou B, Li J, Stevens SM, Romo D, et al. (2013). Interrogating translational efficiency and lineage-specific transcriptomes using ribosome affinity purification. Proc Natl Acad Sci U S A 110, 15395–15400. [PubMed: 24003143]

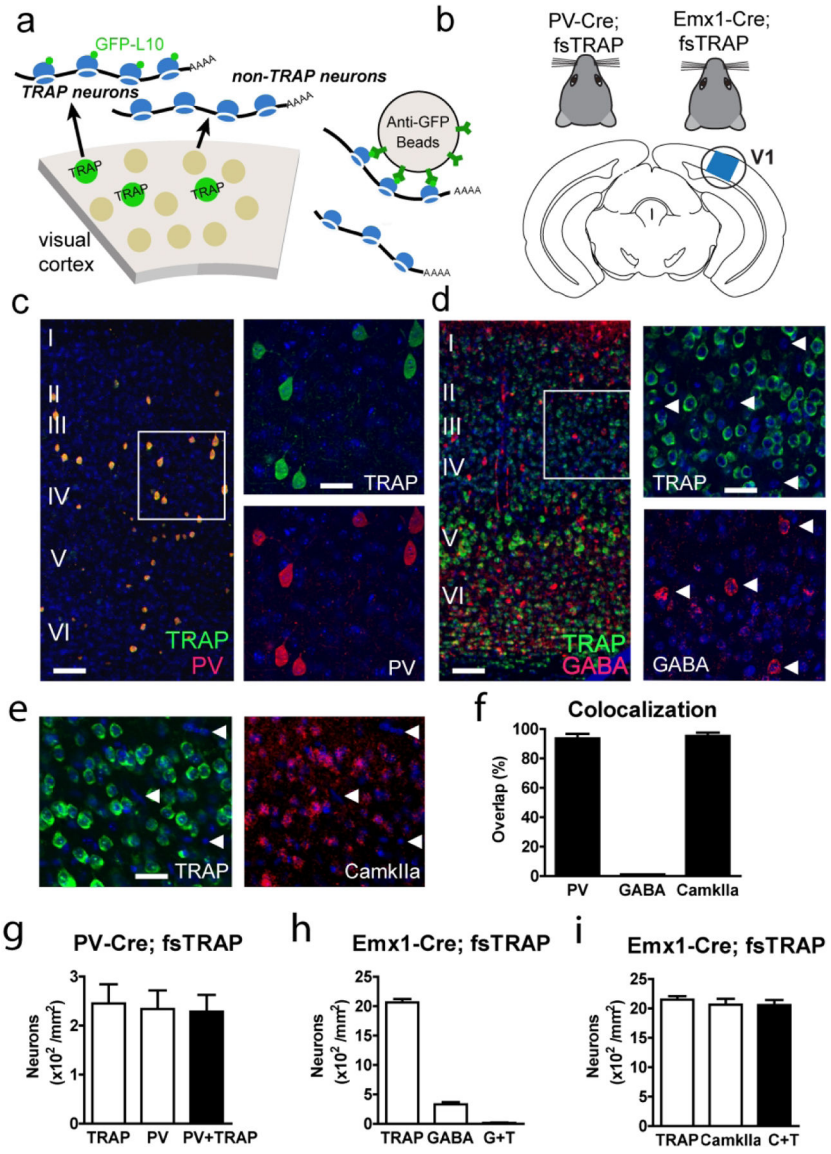

Figure 1. Characterization of PV and Excitatory Neuron Cell Specific fsTRAP Mice

(a) Schematic of the translating ribosome affinity purification (TRAP) strategy (Zhou et al., 2013). Using PV-Cre; fsTRAP or Emx1-Cre; fsTRAP mice, translating polyribosomes (polysomes) from PV or Excitatory neurons (green cells) are EGFP tagged by the EGFP-L10a transgene. Lysis of all cells in the PV-Cre; fsTRAP or Emx1-Cre; fsTRAP cortex releases both tagged and non-tagged polysomes. Only the tagged polysomes are captured on an anti-EGFP affinity matrix and used for purification of PV or Excitatory specific mRNAs. (b) PV and excitatory neurons are harvested from the visual cortices of PV-Cre; fsTRAP or Emx1-Cre; fsTRAP mice at P28. (c) Representative confocal images of genetically labeled PV cells (green), PV immunolabeling (red) and their overlay in layer I-VI of mouse V1 PV-Cre; fsTRAP mice; Scale bar = 100 μm. The white box indicates the region of V1 digitally magnified; Scale bar = 25 μm. Nearly all genetically labeled PV cells are strongly immunopositive for PV. (d) Representative confocal images of genetically labeled excitatory

cells (green), GABA immunolabeling (red) and their overlay in layer I-VI of mouse V1 in Emx1-Cre; fsTRAP mice; Scale bar = 100 μm. The white boxes indicate the region of V1 digitally magnified; Scale bar = 25 μm. Arrowheads indicate GABA immunopositive cells. Nearly all genetically labeled excitatory cells were immunonegative for GABA. (e) Representative confocal images of genetically labeled excitatory cells (green) and CamkIIa immunolabeling (red) from layer II-III of mouse V1 in Emx1-Cre; fsTRAP mice; Scale bar = 25 μm. Nearly all CamkIIa immunonegative cells were also fsTRAP-EGFP negative (arrowheads). (f) Summary of the quantification of genetic and immunolabeling co-localization. (g) All immunopositive PV expressing cells were genetically labeled PV cells across all cortical layers in mouse V1. Overall, there was a trend that 94% ± 3% (mean ± SEM)(not significantly decreased) of all PV-Cre; fsTRAP cells across all the cortical layers are immunopositive for PV. A potential reason is lower detection sensitivity of antibody staining compared with genetic fsTRAP reporter. Another explanation is related to our quantification of robustly stained PV neurons. The quantification is based on the counts of 373 genetically labeled PV cells pooled from 2 sections of 4 different mice. (h) Overall, 1% ± .06% (mean ± SEM) of all Emx1-Cre; fsTRAP cells across all the cortical layers are immunopositive for GABA. The quantification is based on the counts of 3134 genetically labeled excitatory cells and 505 GABA+ cells pooled from 2 sections of 4 different mice. (I) Overall, there was a trend that 95% ± 2% (mean ± SEM)(not significantly reduced) of all Emx1-Cre; fsTRAP cells across all the cortical layers are immunopositive for CamkIIa. The quantification is based on the counts of 2458 genetically labeled excitatory cells pooled from 2 sections of 3 different mice. In (f-i), data represent means ± SEM.

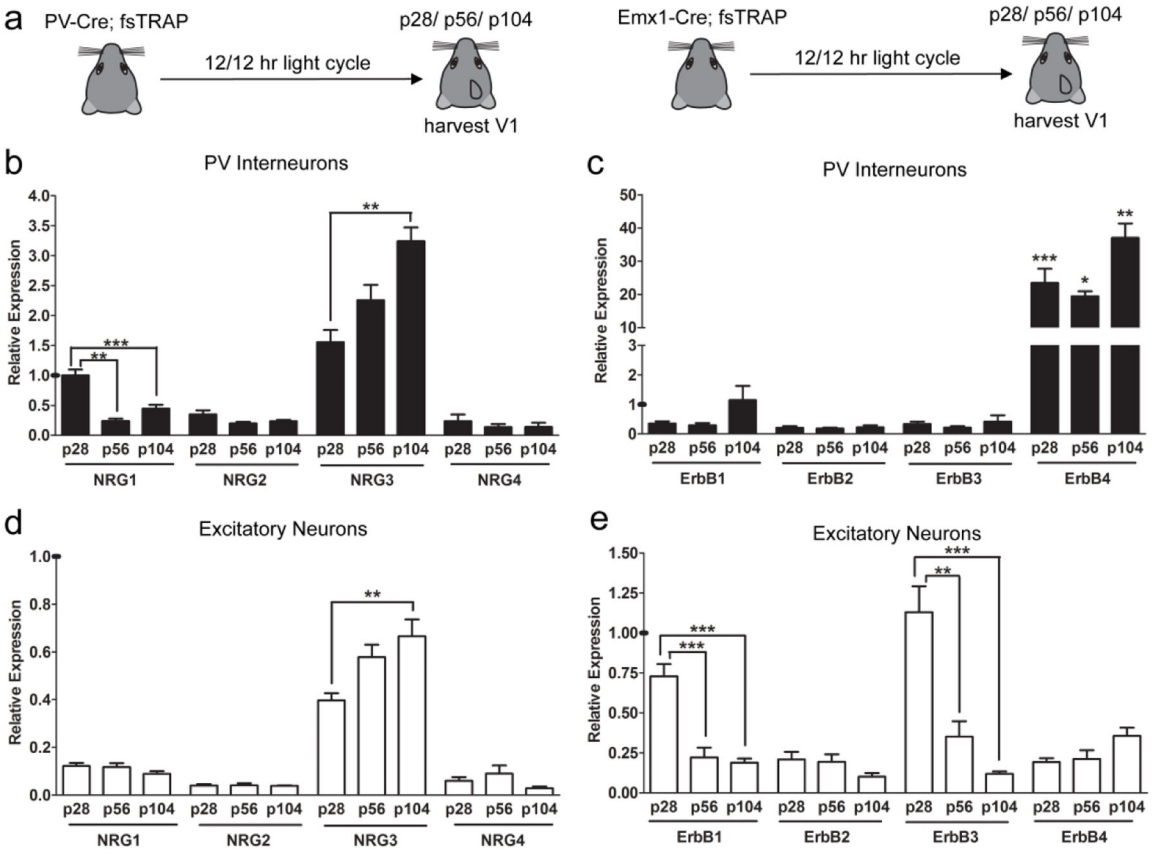

Figure 2. NRG and ErbB Expression by PV and Excitatory Neurons through the Critical Period and into Adulthood

(a) Schematic of the experimental timeline for harvesting visual cortices from PV-Cre; fsTRAP and Emx1-Cre; fsTRAP mice. Mice used for analysis were sacrificed during the critical period at P28, during young adulthood at P56, and during adulthood at P104. (b) PV cell specific (PV-Cre; fsTRAP) mRNA expression levels of *nrg1,2,3,4* mRNA from visual cortices of P28, P56 and P104 mice (n=5–10; (p28)=10, (p56)=5, (p104)=7; n=1 is 5 mice for PV cell specific data; (b-c) represents 25–50 mice per age group). (c) PV cell specific mRNA expression levels of *erbB1,2,3,4* from visual cortices of P28, P56 and P104 mice (n=5–10; (p28)=10, (p56)=5, (p104)=7). (d) Excitatory cell specific (Emx1-Cre; fsTRAP) mRNA expression levels of *nrg1,2,3,4* mRNA from visual cortices of P28, P56 and P104 mice (n=5–10; (p28)=10, (p56=6), (p104)=5; n=1 is 2 mice for excitatory cell specific data; (d-e) represents 10–20 mice per age group). (e) Excitatory cell specific mRNA expression levels of *erbB1,2,3,4* mRNA from visual cortices of P28, P56 and P104 mice (n=5–10; (p28)=10, (p56)=6, (p104)=5). Closed bars=PV cells; Open bars=excitatory cells; all results are analyzed using the ddCt method with *gapdh* as an endogenous control, along with normalization to PV P28 *nrg1* expression, as indicated by a horizontal mark on the y-axis, so that all panels (b, c, d and e) within this figure can be compared. Data represent means ± SEM, *p<0.05. For a summary of statistically significant comparisons see Table 1 (a,b,c).

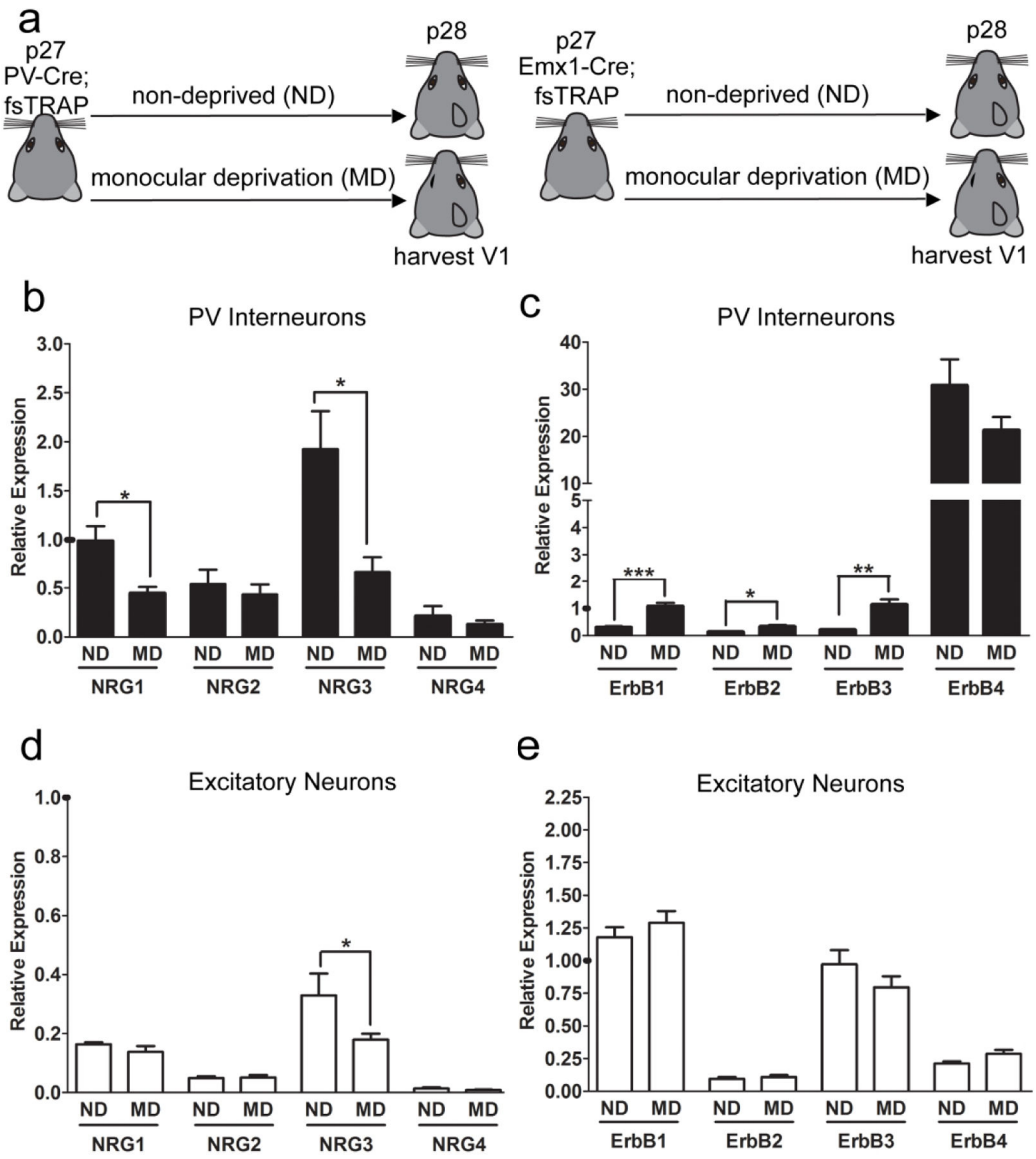

Figure 3. NRG and ErbB Expression by PV and Excitatory Neurons after Monocular Deprivation during the Developmental Critical Period

(a) Schematic of the experimental timeline for monocular deprivation in PV-Cre; fsTRAP and Emx1-Cre; fsTRAP mice and harvesting contralateral visual cortex. Littermates were either reared under normal lighting conditions until P28 or monocularly deprived from P27 to P28. (b) PV cell specific mRNA expression levels of *nrg1,2,3,4* from visual cortices of P28 mice either without deprivation (ND) or after monocular deprivation (MD)(n=5–6; ND=6, MD=5; n=1 is 10 mice for PV cell specific data; (b-c) represents 50–60 mice per group). (c) PV cell specific mRNA expression levels of *erbB1,2,3,4* mRNA from visual cortices of P28 mice either without deprivation or after monocular deprivation (n=5–6; ND=6, MD=5). (d) Excitatory cell specific mRNA expression levels of *nrg1,2,3,4* mRNA from visual cortices of P28 mice either without deprivation or after monocular deprivation (n=5–6; ND=5, MD=6; n=1 is 4 mice for excitatory cell specific data; (d-e) represents 20–24 mice per group). (e) Excitatory cell specific mRNA expression levels of *erbB1,2,3,4* mRNA

from visual cortices of P28 mice either without deprivation or after monocular deprivation (n=5–6; ND=5, MD=6). Closed bars=PV cells; Open bars=excitatory cells; all results are analyzed using the ddCt method with *gapdh* as an endogenous control, along with normalization to PV P28 *nrg1* expression, as indicated by a horizontal mark on the yaxis, so that all panels (b, c, d and e) within this figure can be compared. Data represent means ± SEM, *p<0.05.

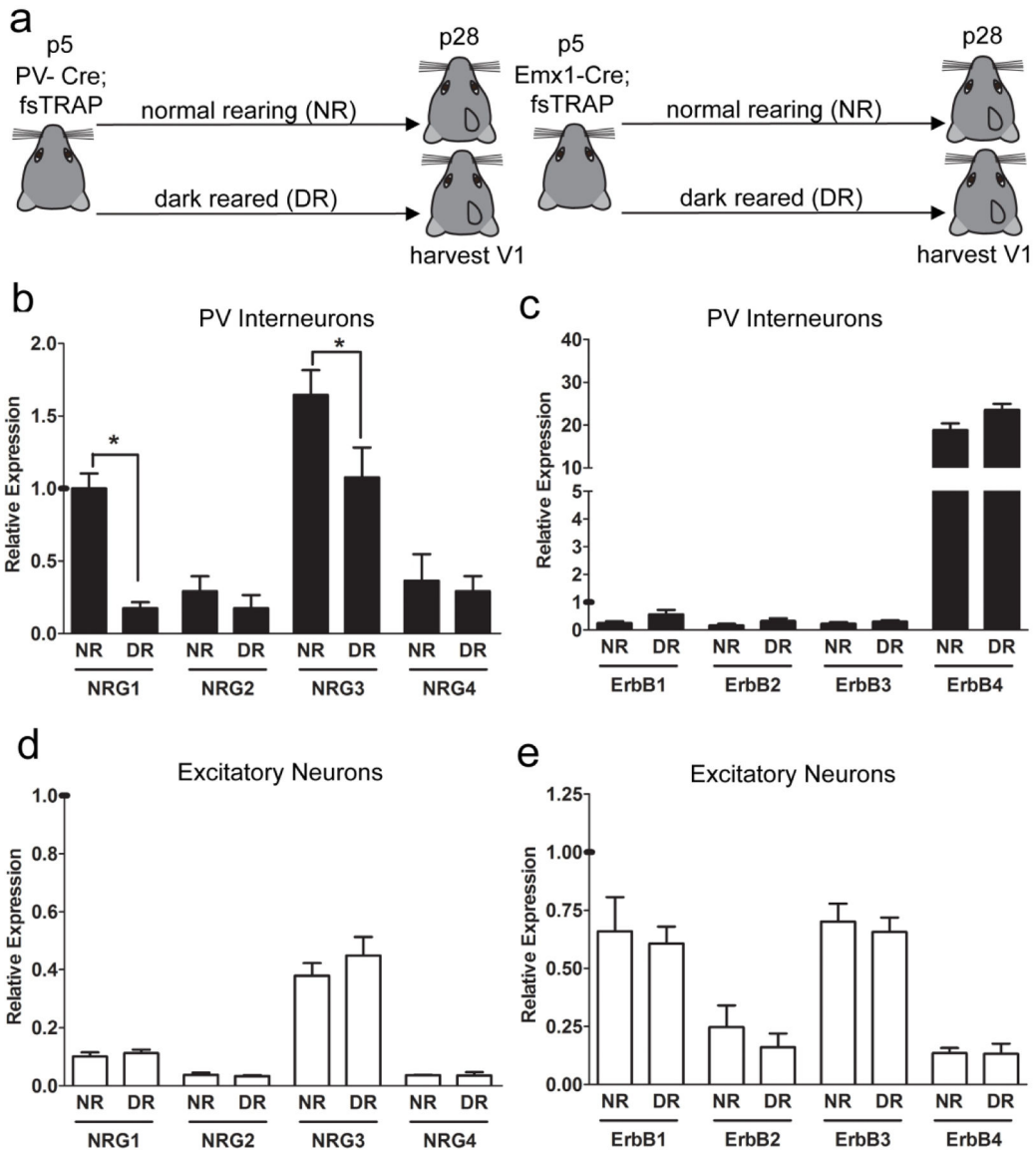

Figure 4. NRG and ErbB Expression by PV and Excitatory Neurons after Dark Rearing during the Developmental Critical Period

(a) Schematic of the experimental timeline for dark rearing PV-Cre; fsTRAP and Emx1-Cre; fsTRAP mice and harvesting visual cortices. Littermates were either reared under normal lighting conditions until P28 or reared in complete darkness from P5 to P28. (b) PV cell specific mRNA expression levels of *nrg1,2,3,4* mRNA from visual cortices of P28 mice either reared normally (NR) or dark reared (DR)(n=5–6; NR=5, DR=6; n=1 is 5 mice for PV cell specific data; (b-c) represents 25–30 mice per rearing group). (c) PV cell specific mRNA expression levels of *erbB1,2,3,4* from visual cortices of P28 mice either reared normally or dark reared (n=5–6; NR=5, DR=6). (d) Excitatory cell specific mRNA expression levels of *nrg1,2,3,4* mRNA from visual cortices of P28 mice either reared normally or dark reared (n=5–7; NR=5, DR=7; n=1 is 2 mice for excitatory cell specific data; (d-e) represents 10–14 mice per rearing group). (e) Excitatory cell specific mRNA expression levels of *erbB1,2,3,4* from visual cortices of P28 mice either reared normally or

dark reared (n=5–7; NR=5, DR=7). Closed bars=PV cells; Open bars=excitatory cells; all results are analyzed using the ddCt method with *gapdh* as an endogenous control, along with normalization to PV P28 *nrg1* expression, as indicated by a horizontal mark on the yaxis, so that all panels (b, c, d and e) within this figure can be compared. Data represent means ± SEM, *$p<0.05$.

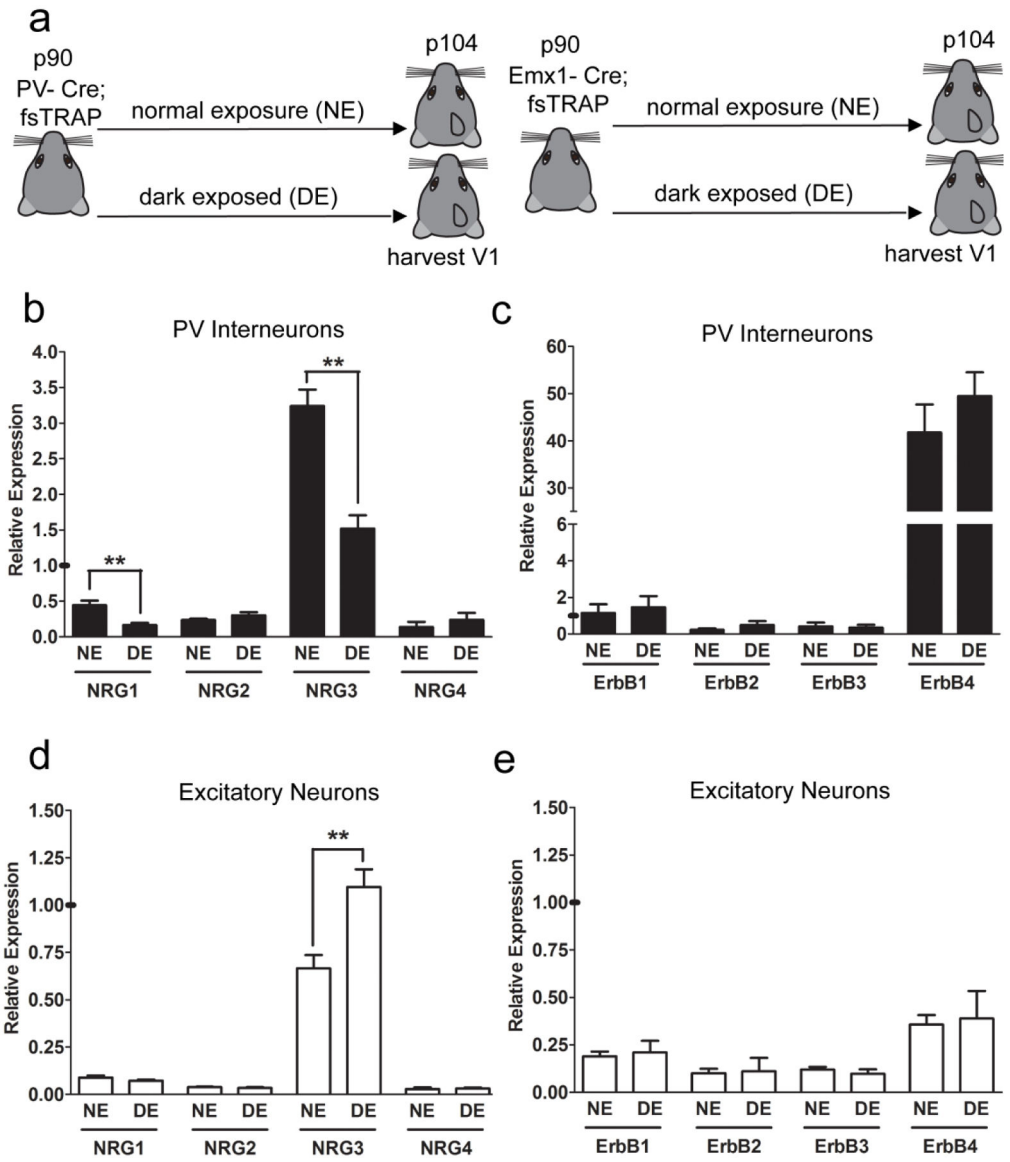

Figure 5. NRG and ErbB Expression by PV and Excitatory Neurons after Dark Exposure during Adulthood

(a) Schematic of the experimental timeline for dark exposing PV-Cre; fsTRAP and Emx1-Cre; fsTRAP mice and harvesting visual cortices. Littermates either remained under normal lighting conditions until P104 or were exposed to complete darkness from P90 to P104. (b) PV cell specific mRNA expression levels of *nrg1,2,3,4* from visual cortices of P104 mice either exposed to normal lighting exposure (NE) or dark exposed (DE)(n=6–7; NE=7, DE=6; n=1 is 5 mice for PV cell specific data; (b-c) represents 30–35 mice per exposure group). (c) PV cell specific mRNA expression levels of *erbB1,2,3,4* mRNA from visual cortices of P104 mice either exposed to normal lighting or dark exposed (n=6–7; NE=7. DE=6). (d) Excitatory cell specific mRNA expression levels of *nrg1,2,3,4* mRNA from visual cortices of P104 mice either exposed to normal lighting or dark exposed (n=5–6; NE=5, DE=6; n=1 is 2 mice for excitatory cell specific data; (d-e) represents 10–12 mice per exposure group). (e) Excitatory cell specific mRNA expression levels of *erbB1,2,3,4* mRNA

from visual cortices of P104 mice either exposed to normal lighting or dark exposed (n=5–6; NE=5, DE=6). Closed bars=PV cells; Open bars=excitatory cells; all results are analyzed using the ddCt method with *gapdh* as an endogenous control, along with normalization to PV P28 *nrg1* expression, as indicated by a horizontal mark on the yaxis, so that all panels (b, c, d and e) within this figure can be compared. Data represent means ± SEM, *p<0.05.

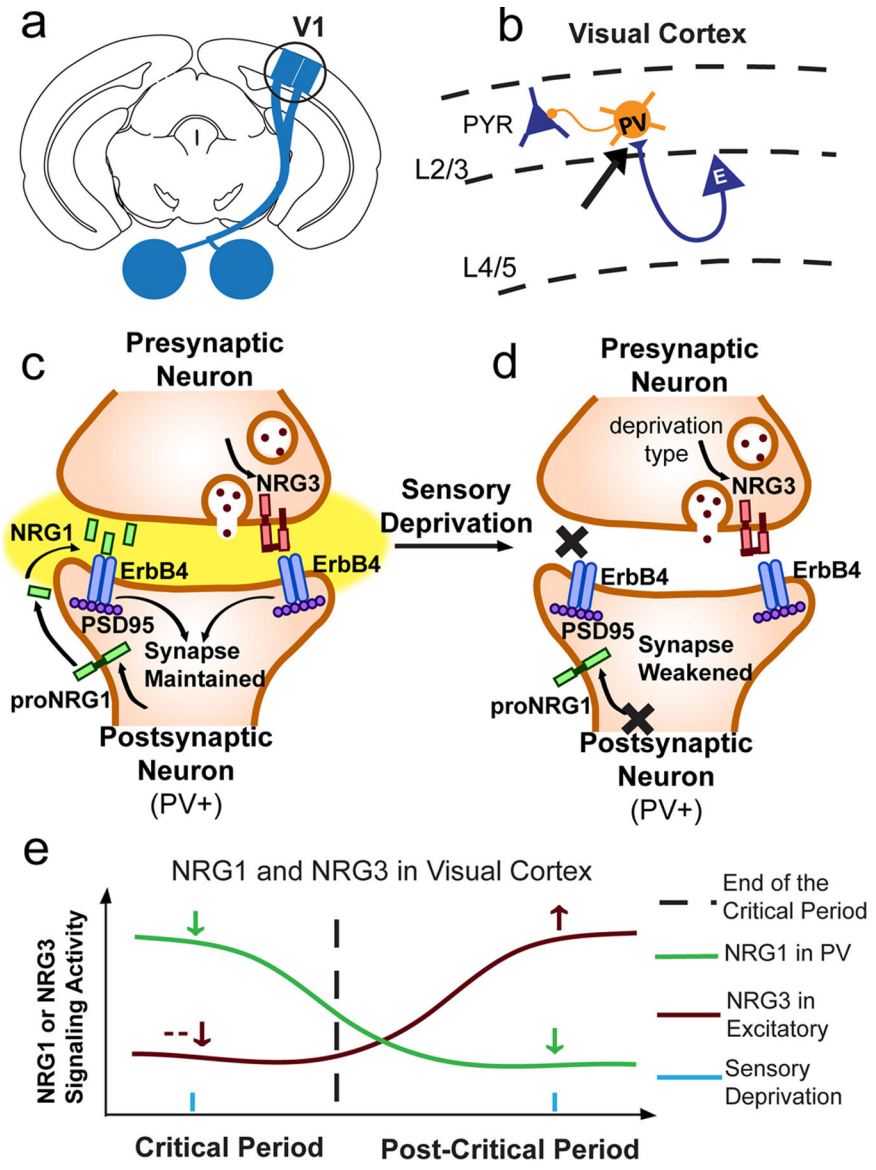

Figure 6. Schematic summary of NRG/ErbB4 signaling by PV interneurons and excitatory neurons and their implications in visual cortical plasticity.

(a) Diagram depicting mouse visual cortex and the associated input from the eyes. (b) A diagram depicting the neural circuit where excitatory inputs from visual cortex layer 4/5 (L4/5) synapse onto PV interneurons in L2/3 (black arrow). PV inhibitory interneurons then synapse onto primary visual L2/3 excitatory pyramidal neurons. (c) A diagram depicting the synapse in B (black arrow). The incoming presynaptic inputs from L4/5 synapse onto a L2/3 PV neuron. Under normal circumstances, NRG1 is expressed, processed, and released from PV neurons in an autonomous manner to bind ErbB4 containing receptors to maintain synaptic strength and inhibition in the cortex. (d) After sensory deprivation, NRG1 levels and ErbB4 signaling (black crosses) are decreased, resulting in weakened synaptic strength and cortical disinhibition. NRG3 levels may depend on the type of sensory deprivation and other cues (age, length/type of deprivation). (e) Model depicting the activities of NRG1 (green) in PV interneurons or NRG3 (maroon) in excitatory neurons before and after the

critical period. With sensory deprivation (blue ticks) NRG1 levels decrease (green arrows), whereas NRG3 levels (maroon arrows) depend on the manipulation. After the critical period (dotted vertical black line), PV NRG1 levels are decreased (green curve), whereas NRG3 levels (maroon curve) in excitatory neurons are increased with age.

Table 1.

NRG and ErbB Expression by PV and Excitatory Neurons through the Critical Period and into Adulthood

a.	PV Interneurons: NRG1,2,3,4 at p28, p56 and p104			
Subject	**Comparison**	**Value ± SEM**	**Value ± SEM**	**Significance Level**
NRG1 ***p<.0005	p28 vs p56	p28= 1 ± .097	p56= .24 ± .038	**p=.002
	p28 vs p104	p28= 1 ± .097	p104= .44 ± .064	***p=.0004
NRG3 **p=.0072	p28 vs p104	p28= 1.56 ± .201	p104= 3.24 ± .23	**p=.003
NRG1–4 (p28) ***p<.0001	NRG1 vs NRG4	NRG1= 1 ± .097	NRG4= .24 ± .11	***p=.0006
	NRG2 vs NRG3	NRG2= .35 ± .069	NRG3= 1.56 ± .20	***p<.0001
	NRG3 vs NRG4	NRG3= 1.56 ± .20	NRG4= .24 ± .11	***p<.0001
NRG1–4 (p56) *p=.024	NRG3 vs NRG4	NRG3= 2.26 ± .26	NRG4= .14 ± .05	*p=.029
NRG1–4 (p104) ***p<.0003	NRG1 vs NRG4	NRG1= .44 ± .064	NRG4= .13 ± .073	**p=.007
	NRG2 vs NRG3	NRG2= .24 ± .020	NRG3= 3.24 ± .23	**p=.0025
	NRG3 vs NRG4	NRG3= 3.24 ± .23	NRG4= .13 ± .073	**p=.0025

b.	Excitatory Neurons: NRG1,2,3,4 at p28, p56 and p104			
Subject	**Comparison**	**Value ± SEM**	**Value ± SEM**	**Significance Level**
NRG3 **p=.0054	p28 vs p104	p28= .40 ± .03	p104= .67 ± .07	**p=0.0027
NRG4 *p=.048	p56 vs p104	p56= .09 ± .03	p104= .03 ± .01	*p=.030
NRG1–4 (p28) ***p<.0001	NRG1 vs NRG2	NRG1= .12 ± .01	NRG2= .04 ± .01	***p<.0001
	NRG2 vs NRG3	NRG2= .04 ± .01	NRG3= .39 ± .03	***p<.0001
	NRG3 vs NRG4	NRG3= .39 ± .03	NRG4= .06 ± .02	***p<.0001
NRG1–4 (p56) ***p<.0006	NRG2 vs NRG3	NRG2= .04 ± .01	NRG3= .58 ± .05	**p=.0022
	NRG3 vs NRG4	NRG3= .58 ± .05	NRG4= .09 ± .03	**p=.0022
NRG1–4 (p104) ***p<.0009	NRG2 vs NRG3	NRG2= .04 ± .001	NRG3= .67 ± .07	**p=.0079
	NRG3 vs NRG4	NRG3= .67 ± .07	NRG4= .03 ± .01	**p=.0079

c.	Excitatory Neurons: ErbB1,2,3,4 at p28, p56 and p104			
Subject	**Comparison**	**Value ± SEM**	**Value ± SEM**	**Significance Level**
ErbB1 ***p=.0009	p28 vs p56	p28= .73 ± .08	p56= .22 ± .06	***p=.001
	p28 vs p104	p28= .73 ± .08	p104= .19 ± .06	***p=.0007
ErbB3 **p=.0012	p28 vs p56	p28= 1.13 ± .16	p56= .35 ± .09	**p=.0016
	p28 vs p104	p28= 1.13 ± .16	p104= .12 ± .01	***p=.001
ErbB1–4 (p28) ***p<.0001	ErbB1 vs ErbB2	ErbB1= .73 ± .08	ErbB2= .21 ± .05	***p<.0001
	ErbB1 vs ErbB4	ErbB1= .73 ± .08	ErbB4= .19 ± .03	***p<.0001
	ErbB2 vs ErbB3	ErbB2= .21 ± .05	ErbB3= 1.13 ± .16	***p<.0001
	ErbB3 vs ErbB4	ErbB3= 1.13 ± .16	ErbB4= .19 ± .03	***p<.0001
ErbB1–4 (p104) **p<.0059	ErbB2 vs ErbB4	ErbB2= .10 ± .02	ErbB4= .36 ± .05	*p=.0159

c.	Excitatory Neurons: ErbB1,2,3,4 at p28, p56 and p104			
Subject	**Comparison**	**Value ± SEM**	**Value ± SEM**	**Significance Level**
	ErbB3 vs ErbB4	ErbB3= .12 ± .01	ErbB4= .36 ± .05	**p=.0079

Note that for Table 1 (a,b,c) the results (p-values) of one-way ANOVA Kruskal Wallis tests are listed in the Subject columns. The results of Mann-Whitney U tests for individual comparisons are listed in the Significance Level columns. A p-value of <%0.05 was considered statistically significant, and all significant results are shown